Electronic Supplementary Information

{$Gd_{44}Ni_{22}$}: A Gigantic 3*d*-4*f* Wheel-like Cluster with Large Magnetocaloric Effect

Zixiu Lu,[ab] Zhu Zhuo,[cd] Wei Wang,[cd*] You-Gui Huang,[cd*] and Maochun Hong[abd]

[a] Ganjiang Innovation Academy, Chinese Academy of Sciences, Ganzhou 341000, China

[b] School of Rare Earth, University of Science and Technology of China, Hefei, China.

[c] CAS Key Laboratory of Design and Assembly of Functional Nanostructures, and Fujian Provincial Key Laboratory of Nanomaterials, Fujian Institute of Research on the Structure of Matter, Chinese Academy of Sciences, China

[d] Xiamen Key Laboratory of Rare Earth Photoelectric Functional Materials, Xiamen Institute of Rare Earth Materials, Haixi Institutes, Chinese Academy of Sciences, Xiamen, Fujian 361021, China;

[e] Fujian Science & Technology Innovation Laboratory for Optoelectronic Information of China, Fuzhou, 350108

*Corresponding author:

Wei Wang: wangwei@fjirsm.ac.cn;

You-Gui Huang: yghuang@fjirsm.ac.cn.

Contents

1. Materials and Measurements

1.1 Chemicals and Physical Measurements.

Commercial chemicals, $Gd(NO_3)_3·6H_2O$ (Adamas Co., Ltd., >99.0 %), $Ni(NO_3)_2·6H_2O$ (Adamas Co., Ltd., 99.99 %), NaOH (Greagent Co., Ltd., 96.0 %), 3-Hydroxy-2-(hydroxymethyl)-2-methylpropanoic acid (H_3dmpa, Bide Co., Ltd., 95.0 %) and Iminodiacetic acid (IDA, Bide Co., Ltd., 98.0 %) were used as received without further purification. NaOH (3.0 mol/L, 250 ml) was prepared using conventional methods. Infrared spectrum was recorded on a Thermo Nicolet iS 50 spectrophotometers. Thermogravimetric analysis (TGA) curve was carried out under nitrogen with a heating rate of 10 ℃/min using Mettler Telodo TGA/DSC-1 thermal analyzer. Powder X-ray diffraction data (PXRD) was recorded on a Miniflex 600 powder X-ray diffractometer (Cu $K\alpha$, λ = 1.54184 Å) in the 2θ range of 3–50° at room temperature. Magnetic susceptibility was measured using a Quantum Design MPMS superconducting quantum interference device (SQUID). Diamagnetic corrections were made with Pascal's constants. The magnetic susceptibility was performed in 2–300 K under a dc field of 1000 Oe. The isothermal magnetization was measured at 2–10 K in applied field of 0–7 T. The M–H curves at each temperature were measured with step size of 1000 Oe during 0–2 T and that of 2000 Oe during 2–7 T.

1.2 Synthesis of $[Gd_{44}Ni_{22}(CO_3)_{16}(NO_3)_4(H_2O)_{58}(\mu_3\text{-}OH)_{76}(\mu_2\text{-}O)_6(IDA)_{28}(H_2dmpa)_2]·(H_2O)_x$ (1, x ≈ 118).

Hydroxy-2-(hydroxymethyl)-2-methylpropanoic acid (H_3dmpa, 0.1251 g, 0.93 mmol), Iminodiacetic acid (IDA, 0.1290 g, 0.97 mmol), $Gd(NO_3)_3·6H_2O$ (1.0769 g, 2.39 mmol), and $Ni(NO_3)_2·4H_2O$ (0.6983 g, 2.40 mmol) were dissolved in the 10 ml H_2O. This solution was stirred for 24 h and then a freshly prepared NaOH solution (aq. 3.0 M) drop wised to the mixture to the point of incipient but permanent precipitation (PH≈6). The mixture solution was filtered and sealed in a 25 mL Teflon-lined stain less steel vessel and heated at 140 °C for 4 days. At a rate of 5 °C/h, the system was

allowed to cool to room temperature. Evaporation of the filtrate in a beaker under ambient conditions afforded the block-shaped light green crystals of **1** after about 20 days (yield 50 % based on Gd^{3+}). Elemental analysis calcd (%) for **1**: C 9.73, H 3.54, N 2.79; Found: C 9.62, H 2.60, N 2.69. IR (KBr, cm-1): 3241 (m), 1577 (s), 1504 (w), 1458 (w), 1412 (s), 1316 (w), 1087 (w), 932 (w), 827 (w), 717 (w).

1.3 X-ray Crystallography.

Single-crystal X-ray diffraction data of **1** were collected at 200(2) K on the Bruker SMART diffractometer with monochromatic Mo *Kα* radiation (λ = 0.71073 Å). The structure was solved by direct methods and all non-H atoms were subjected to anisotropic refinement by full-matrix least-squares refinement on F^2 using using SHELXL−2018 within Olex2.[1,2] All non-hydrogen atoms were refined anisotropically. The hydrogen atoms of organic ligand were generated geometrically (C−H = 0.96 Å, N−H = 0.90 Å). The contribution of the disordered solvent molecules was subtracted from the reflection data by the SQUEEZE method as implanted in PLATON program.[3−6] There are 39 disordered water molecules per formula were removed by SQUEEZE in the refinement, but accurately confirmed by TG, elemental analyses and charge balance. Refinement parameters and crystallographic data for **1** are shown in Table S1−S2. CCDC-2208968 contains the supplementary crystallographic data. This data can be obtained free of charge via www.ccdc.cam.ac.uk/data_request/cif.

2. Supplementary Tables

Table S1. Crystallographic Data and Structure Refinements for **1**.

Complex	{$Gd_{44}Ni_{22}$} (**1**)
formula	$Gd_{44}Ni_{22}C_{130}N_{32}O_{314}H_{356}$
fw	15603.07
crystal system	Monoclinic
space group	$P2_1/n$
a, Å	20.2655(2)
b, Å	34.6370(6)
c, Å	40.1162(4)
α, deg	90
β, deg	91.9750(10)
γ, deg	90
V, Å^3	28142.3(6)
Z	2
D_c / g cm^{-3}	1.841
T, K	200.00
F(000)	145608.0
reflections collected / unique	182894 /51512
R_{int}	0.0909
GOF on F^2	1.102
R_1, wR_2 $I>2\sigma(I)$[a]	0.0668, 0.1892
R_1, wR_2 (all data)	0.0870, 0.1991
CCDC Number	2208968

[a] $R_1 = \Sigma||F_o| - |F|| / \Sigma|F_o|$ and $wR_2 = [\Sigma w(F_o^2 - F_c^2)^2 / \Sigma wF_o^4]^{1/2}$ for $F_o^2 > 2\sigma(F_o^2)$

Table S2. Selected bond lengths [Å] for **1**.

Gd(1)-O(4)	2.390(6)	Gd(12)-O(60)	2.539(7)	Ni(1)-N(8)	2.038(10)
Gd(1)-O(6)	2.450(8)	Gd(12)-O(80)	2.417(7)	Ni(2)-O(64)	2.017(8)
Gd(1)-O(14)	2.393(7)	Gd(12)-O(82)	2.348(6)	Ni(2)-O(94)	2.056(8)
Gd(1)-O(18)	2.388(7)	Gd(12)-O(108)	2.293(6)	Ni(2)-O(132)	2.032(8)
Gd(1)-O(24)	2.375(6)	Gd(12)-O(114)	2.540(7)	Ni(2)-N(17)	2.102(11)
Gd(1)-O(40)	2.433(7)	Gd(12)-O(134)	2.588(8)	Ni(2)-O(127)	2.038(10)
Gd(1)-O(46)	2.444(7)	Gd(12)-O(95)	2.425(8)	Ni(2)-O(37)	2.058(10)

Gd(1)-O(82)	2.405(7)	Gd(13)-O(44)#1	2.482(7)	Ni(3)-O(32)	2.046(7)
Gd(1)-O(104)	2.425(7)	Gd(13)-O(76)	2.355(8)	Ni(3)-O(50)	2.041(9)
Gd(2)-O(62)	2.672(8)	Gd(13)-O(78)	2.442(7)	Ni(3)-O(92)	2.025(9)
Gd(2)-O(84)	2.358(7)	Gd(13)-O(100)#1	2.487(8)	Ni(3)-O(136)	2.052(7)
Gd(2)-O(116)	2.381(8)	Gd(13)-O(41)#1	2.433(8)	Ni(3)-O(81)	2.045(7)
Gd(2)-O(118)	2.319(8)	Gd(13)-O(99)	2.390(8)	Ni(3)-N(16)	2.082(9)
Gd(2)-O(128)	2.430(8)	Gd(13)-O(103)	2.483(9)	Ni(4)-O(10)	2.042(7)
Gd(2)-O(140)	2.707(8)	Gd(13)-O(107)	2.416(10)	Ni(4)-O(54)	2.071(7)
Gd(2)-O(83)	2.308(8)	Gd(13)-O(117)	2.659(12)	Ni(4)-O(96)	1.991(8)
Gd(2)-O(89)	2.433(8)	Gd(14)-O(38)	2.386(7)	Ni(4)-O(102)	2.095(8)
Gd(2)-O(129)	2.499(14)	Gd(14)-O(66)	2.457(8)	Ni(4)-O(79)	2.045(8)
Gd(3)-O(22)	2.540(7)	Gd(14)-O(98)	2.431(8)	Ni(4)-N(6)	2.039(10)
Gd(3)-O(36)#1	2.344(8)	Gd(14)-O(138)	2.496(7)	Ni(5)-O(100)	2.028(8)
Gd(3)-O(76)	2.504(8)	Gd(14)-O(142)	2.334(6)	Ni(5)-O(112)	2.058(8)
Gd(3)-O(78)	2.370(7)	Gd(14)-O(5)	2.501(7)	Ni(5)-O(41)	2.032(9)
Gd(3)-O(150)	2.316(8)	Gd(14)-O(43)	2.262(7)	Ni(5)-O(27)	2.030(9)
Gd(3)-O(154)	2.393(7)	Gd(14)-O(23)	2.421(8)	Ni(5)-O(29)	2.055(10)
Gd(3)-O(3)	2.421(9)	Gd(14)-O(49)	2.610(8)	Ni(5)-N(5)	2.111(11)
Gd(3)-O(25)#1	2.401(9)	Gd(15)-O(108)	2.417(8)	Ni(6)-O(28)	2.102(7)
Gd(3)-O(143)	2.94(2)	Gd(15)-O(134)	2.373(7)	Ni(6)-O(30)	2.080(8)
Gd(4)-O(1)	2.493(7)	Gd(15)-O(91)	2.497(8)	Ni(6)-O(74)	2.026(8)
Gd(4)-O(4)	2.433(6)	Gd(15)-O(51)	2.399(8)	Ni(6)-O(138)	2.055(7)
Gd(4)-O(16)	2.528(7)	Gd(15)-O(111)	2.444(8)	Ni(6)-O(142)	2.006(7)
Gd(4)-O(32)	2.350(8)	Gd(15)-O(61)	2.472(9)	Ni(6)-N(4)	2.077(10)
Gd(4)-O(34)	2.495(8)	Gd(15)-O(63)	2.425(9)	Ni(7)-O(26)	2.045(7)
Gd(4)-O(40)	2.354(7)	Gd(15)-O(2)	2.388(11)	Ni(7)-O(72)	2.069(8)
Gd(4)-O(88)	2.449(7)	Gd(15)-O(139)	2.587(15)	Ni(7)-O(80)	2.036(7)
Gd(4)-O(152)	2.485(7)	Gd(16)-O(20)#1	2.333(7)	Ni(7)-O(86)	2.026(8)
Gd(4)-O(81)	2.446(7)	Gd(16)-O(22)	2.345(7)	Ni(7)-O(13)	2.094(7)
Gd(5)-O(110)	2.462(9)	Gd(16)-O(36)#1	2.457(7)	Ni(7)-N(14)	2.156(12)
Gd(5)-O(118)	2.361(8)	Gd(16)-O(56)#1	2.437(7)	Ni(8)-O(60)	2.037(7)
Gd(5)-O(128)	2.294(9)	Gd(16)-O(64)	2.424(7)	Ni(8)-O(82)	1.983(7)
Gd(5)-O(31)	2.204(13)	Gd(16)-O(94)	2.440(7)	Ni(8)-O(104)	2.046(7)
Gd(5)-O(129)	2.881(13)	Gd(16)-O(126)#1	2.529(7)	Ni(8)-O(144)	2.089(7)
Gd(5)-O(71)	2.275(17)	Gd(16)-O(157)#1	2.550(7)	Ni(8)-O(148)	2.064(8)
Gd(5)-O(151)	2.35(3)	Gd(16)-O(101)	2.483(9)	Ni(8)-N(1)	2.071(9)
Gd(5)-O(19)	2.72(2)	Gd(17)-O(78)	2.428(7)	Ni(9)-O(66)	2.062(7)
Gd(6)-O(10)	2.435(8)	Gd(17)-O(154)	2.422(7)	Ni(9)-O(98)	2.009(8)
Gd(6)-O(20)	2.411(7)	Gd(17)-O(99)	2.361(8)	Ni(9)-O(87)	2.029(9)
Gd(6)-O(38)	2.372(6)	Gd(17)-O(105)	2.377(10)	Ni(9)-O(97)	2.063(8)
Gd(6)-O(56)	2.400(7)	Gd(17)-O(113)#1	2.352(10)	Ni(9)-O(59)	2.067(8)
Gd(6)-O(58)	2.412(7)	Gd(17)-O(135)	2.519(13)	Ni(9)-N(11)	2.117(10)
Gd(6)-O(68)	2.351(7)	Gd(17)-O(143)	2.387(15)	Ni(10)-O(20)	2.014(7)
Gd(6)-O(74)	2.443(7)	Gd(17)-O(145)	2.412(14)	Ni(10)-O(58)	2.068(8)
Gd(6)-O(96)	2.410(7)	Gd(18)-O(1)	2.314(7)	Ni(10)-O(70)	2.063(8)
Gd(6)-O(142)	2.420(7)	Gd(18)-O(42)	2.422(7)	Ni(10)-O(157)	2.008(8)
Gd(7)-O(98)	2.383(7)	Gd(18)-O(62)	2.494(7)	Ni(10)-O(85)$^{\#1}$	2.015(8)
Gd(7)-O(110)	2.333(8)	Gd(18)-O(84)	2.364(7)	Ni(10)-N(10)	2.071(10)
Gd(7)-O(116)	2.363(7)	Gd(18)-O(90)	2.468(8)	Ni(11)-O(18)	1.996(6)

Gd(7)-O(118)	2.401(8)	Gd(18)-O(152)	2.564(7)	Ni(11)-O(46)	2.053(8)
Gd(7)-O(146)	2.472(9)	Gd(18)-O(156)	2.533(9)	Ni(11)-O(106)	2.077(9)
Gd(7)-O(5)	2.444(7)	Gd(18)-O(89)	2.406(9)	Ni(11)-O(122)	2.029(8)
Gd(7)-O(93)	2.443(7)	Gd(18)-N(13)	2.561(10)	Ni(11)-O(45)	2.048(8)
Gd(7)-O(97)	2.434(8)	Gd(19)-O(119)	2.427(10)	Ni(11)-N(12)	2.071(9)
Gd(8)-O(14)	2.450(7)	Gd(19)-O(15)	2.592(12)	Gd(2)-Gd(21)	3.6313(14)
Gd(8)-O(18)	2.355(7)	Gd(19)-O(121)	2.372(11)	Gd(2)-Gd(5)	3.6175(13)
Gd(8)-O(22)	2.356(7)	Gd(19)-O(125)	2.357(10)	Gd(3)-Gd(13)	3.9330(8)
Gd(8)-O(64)	2.412(7)	Gd(19)-O(67)	2.455(11)	Gd(3)-Gd(17)	3.7495(8)
Gd(8)-O(122)	2.549(7)	Gd(19)-O(17)	2.498(13)	Gd(7)-Gd(2)	3.7546(8)
Gd(8)-O(130)	2.546(7)	Gd(19)-O(69)	2.428(14)	Gd(7)-Gd(5)	3.8826(14)
Gd(8)-O(132)	2.474(7)	Gd(19)-O(35)	2.480(13)	Gd(8)-Gd(16)	3.8300(9)
Gd(8)-O(150)	2.454(7)	Gd(19)-O(73)	2.414(13)	Gd(11)-Gd(7)	3.8326(7)
Gd(8)-O(55)	2.462(9)	Gd(20)-O(72)	2.387(8)	Gd(11)-Gd(2)	3.6592(8)
Gd(9)-O(43)	2.426(9)	Gd(20)-O(80)	2.400(7)	Gd(11)-Gd(5)	3.9706(14)
Gd(9)-O(49)	2.348(7)	Gd(20)-O(84)	2.343(7)	Gd(13)-Gd(17)	3.8977(9)
Gd(9)-O(109)	2.469(8)	Gd(20)-O(90)	2.331(7)	Gd(18)-Gd(20)	3.8247(7)
Gd(9)-O(7)	2.467(10)	Gd(20)-O(114)	2.430(7)	Gd(18)-Gd(2)	3.6506(7)
Gd(9)-O(57)	2.382(9)	Gd(20)-O(83)	2.384(8)	Gd(18)-Gd(21)	3.9519(14)
Gd(9)-C(64)	2.893(15)	Gd(20)-O(21)	2.463(9)	Gd(20)-Gd(2)	3.7564(8)
Gd(9)-O(131)	2.481(13)	Gd(20)-O(11)	2.414(7)	Gd(20)-Gd(21)	3.8920(15)
Gd(9)-O(33)	2.445(12)	Gd(21)-O(90)	2.455(8)	Gd(22)-Gd(3)	3.9325(8)
Gd(9)-O(147)	2.377(14)	Gd(21) -O(83)	2.369(8)	Gd(22)-Gd(13)	3.7454(9)
Gd(10)-O(8)	2.488(7)	Gd(21) -O(89)	2.244(8)	Gd(22)-Gd(17)	3.8591(8)
Gd(10)-O(44)	2.506(8)	Gd(21) -O(65)	2.198(14)	Gd(1)-Ni(1)	3.4641(14)
Gd(10)-O(54)	2.503(8)	Gd(21) -O(141)	2.277(19)	Gd(1)-Ni(8)	3.4572(16)
Gd(10)-O(68)	2.471(7)	Gd(21) -O(149)	2.665(17)	Gd(1)-Ni(11)	3.4525(15)
Gd(10)-O(96)	2.378(7)	Gd(21) -O(75)	2.300(3)	Gd(4)-Ni(1)	3.5241(15)
Gd(10)-O(100)	2.367(7)	Gd(21) -O(153)	2.590(3)	Gd(4)-Ni(3)	3.4548(14)
Gd(10)-O(112)	2.437(7)	Gd(22)-O(16)	2.481(7)	Gd(6)-Ni(4)	3.4656(15)
Gd(10)-O(120)	2.480(8)	Gd(22)-O(32)	2.474(8)	Gd(6)-Ni(6)	3.4616(16)
Gd(10)-O(115)	2.432(8)	Gd(22)-O(50)	2.412(8)	Gd(6)-Ni(10)	3.4605(15)
Gd(11)-O(8)	2.284(7)	Gd(22)-O(76)	2.380(7)	Gd(7)-Ni(9)	3.5273(16)
Gd(11)-O(48)	2.445(7)	Gd(22)-O(124)	2.447(8)	Gd(8)-Ni(2)	3.5099(17)
Gd(11)-O(110)	2.477(8)	Gd(22)-O(154)	2.419(7)	Gd(10)-Ni(4)	3.5301(15)
Gd(11)-O(116)	2.377(7)	Gd(22)-O(47)	2.427(8)	Gd(10)-Ni(5)	3.4536(16)
Gd(11)-O(120)	2.569(8)	Gd(22)-O(99)	2.406(8)	Gd(12)-Ni(8)	3.5381(15)
Gd(11)-O(128)	2.376(9)	Gd(22)-O(117)	2.597(11)	Gd(12)-Ni(7)	3.4923(17)
Gd(11)-O(140)	2.504(8)	Ni(1)-O(6)	2.041(7)	Gd(13)-Ni(5)$^{\#1}$	3.5252(19)
Gd(11)-O(53)	2.593(10)	Ni(1)-O(12)	2.015(7)	Gd(14)-Ni(6)	3.5362(15)
Gd(11)-N(3)	2.571(10)	Ni(1)-O(34)	2.064(7)	Gd(14)-Ni(9)	3.4878(18)
Gd(12)-O(24)	2.376(7)	Ni(1)-O(40)	2.004(7)	Gd(16)-Ni(2)	3.5193(17)
Gd(12)-O(26)	2.455(7)	Ni(1)-O(52)	2.089(7)	Gd(20)-Ni(7)	3.5178(16)

Symmetry transformations used to generate equivalent atoms:

#1 –x+1, −y+1, −z+1

Table S3. Selected BVS calculations for Ni, C (in CO_3^{2-}), N (in NO_3^-), and O atoms in **1**.

Atom	N8	O12	O34	O40	O52	O6	Σcation
Ni1	0.34	0.37	0.33	0.38	0.31	0.35	2.08
Atom	N17	O127	O132	O37	O64	O94	Σcation
Ni2	0.29	0.36	0.36	0.33	0.37	0.34	2.05
Atom	N16	O136	O32	O50	O81	O92	Σcation
Ni3	0.31	0.34	0.35	0.35	0.35	0.37	2.07
Atom	N6	O10	O102	O54	O79	O96	Σcation
Ni4	0.35	0.35	0.30	0.32	0.35	0.40	2.07
Atom	N5	O100	O112	O27	O29	O41	Σcation
Ni5	0.29	0.36	0.33	0.36	0.34	0.36	2.05
Atom	N4	O138	O142	O28	O30	O74	Σcation
Ni6	0.32	0.34	0.39	0.30	0.32	0.37	2.02
Atom	N14	O13	O26	O72	O80	O86	Σcation
Ni7	0.25	0.30	0.35	0.33	0.35	0.36	1.95
Atom	N1	O104	O144	O148	O60	O82	Σcation
Ni8	0.32	0.35	0.31	0.33	0.35	0.41	2.06
Atom	N11	O59	O66	O87	O97	O98	Σcation
Ni9	0.28	0.33	0.33	0.36	0.33	0.38	2.02
Atom	N10	O157	O20	O58	O70	O85	Σcation
Ni10	0.32	0.38	0.38	0.33	0.33	0.38	2.11
Atom	N12	O106	O122	O18	O45	O46	Σcation
Ni11	0.32	0.32	0.36	0.40	0.35	0.34	2.08
Atom	N12	O106	O122	O18	O45	O46	Σcation
Ni11	0.32	0.32	0.36	0.40	0.35	0.34	2.08
Atom	O4	O114	O1	—	—	—	Σcation
C1	1.44	1.37	1.23	—	—	—	4.04
Atom	O16	O150	O14	—	—	—	Σcation
C4	1.42	1.38	1.25	—	—	—	4.05
Atom	O130	O134	O24	—	—	—	Σcation
C8	1.41	1.33	1.21	—	—	—	3.95
Atom	O44	O56	O36	—	—	—	Σcation
C9	1.35	1.37	1.30	—	—	—	4.02
Atom	O68	O5	O8	—	—	—	Σcation
C12	1.32	1.42	1.15	—	—	—	3.89
Atom	O126	O49	O38	—	—	—	Σcation
C32	1.47	1.26	1.23	—	—	—	3.96
Atom	O108	O91	O86	—	—	—	Σcation
C38	1.32	1.29	1.32	—	—	—	3.93
Atom	O87	O7	O43	—	—	—	Σcation
C64	1.43	1.31	1.19	—	—	—	3.93
Atom	O155	O39	O77	—	—	—	Σcation
N2	1.51	1.65	1.78	—	—	—	4.94
Atom	O17	O137	O15	—	—	—	Σcation
N7	1.61	1.61	1.71	—	—	—	4.93

Atom	O155	O39	O77	—	—	—	Σcation
N15	1.83	1.25	1.82	—	—	—	4.90
Atom	Gd13	Gd22	—	—	—	—	Σcation
O117	0.18	0.22	—	—	—	—	0.40
Atom	Gd5	Gd21	Gd2	—	—	—	Σcation
O129	0.10	0.06	0.28	—	—	—	0.44
Atom	Gd17	Gd3	—	—	—	—	Σcation
O143	0.38	0.08	—	—	—	—	0.46

*The bond valence was calculated by the equation: $S = \exp((R_0 - R)/b)$ where where S is the experimental bond valence, R the observed bond length, and R_0 and b are fitted bond valence parameters. R_0 of Ni–O, Ni–N, C–O, N–O are 1.654, 1.647, 1.390, 1.432 and $b = 0.37$. Bond valence sum (BVS) calculations were performed for selected atoms of the asymmetric unit (Ni, 1.95–2.11; C, 3.89–4.05; N, 4.90–4.94), which are consistent with the expected valence values (+2; +4; +5) and confirm the reliability of the structure.

Table S4. Magnetic entropy changes for selected high-nuclearity Gd^{III} -based cluster materials.

Compound	$-\Delta S_{max}$ ($J \cdot kg^{-1} \cdot K^{-1}$)	T (K)	ΔH (T)	Ref
$\{Gd_{60}\}$	48.0	2.0	7	[7]
$\{Gd_{104}\}$	46.9	2	7	[8]
$\{Gd_{24}\}$	46.1	2.5	7	[9]
$\{Gd_{48}\}$	43.6	1.8	7	[10]
$\{Gd_{27}\}$	41.8	2.0	7	[11]
$\{Gd_{36}\}$	39.7	2.5	7	[12]
$\{Gd_{37}\}$	38.7	2.0	7	[13]
$\{Gd_{140}\}$	38.0	2.0	7	[14]
$\{Gd_{38}\}$	37.9	1.8	7	[15]
$\{Gd_{158}Co_{38}\}$	46.9	2	7	[16]
$\{Gd_{44}Ni_{22}\}$	44.9	2	7	This work
$\{Gd_{30}Co_{12}\}$	44.7	2.0	7	[17]
$\{Gd_{96}Ni_{64}\}$	42.8	3.0	7	[18]
$\{Gd_{102}Ni_{36}\}$	41.3	2.0	7	[19]
$\{Gd_{42}Co_{10}\}$	41.3	2.0	7	[20]

{$Gd_{78}Ni_{64}$}	40.6	3.0	7	[21]
{$Gd_{52}Ni_{56}$}	40.5	3.0	7	[22]
{$Gd_{45}Co_{7}$}	40.5	2.0	7	[23]
{$Gd_{42}Ni_{10}$}	38.2	2.0	7	[20]
{$Gd_{24}Co_{16}$}	26.0	3.8	7	[24]
{$Gd_{24}Cu_{36}$}	21.0	2.1	7	[25]

3. Supplementary Figures

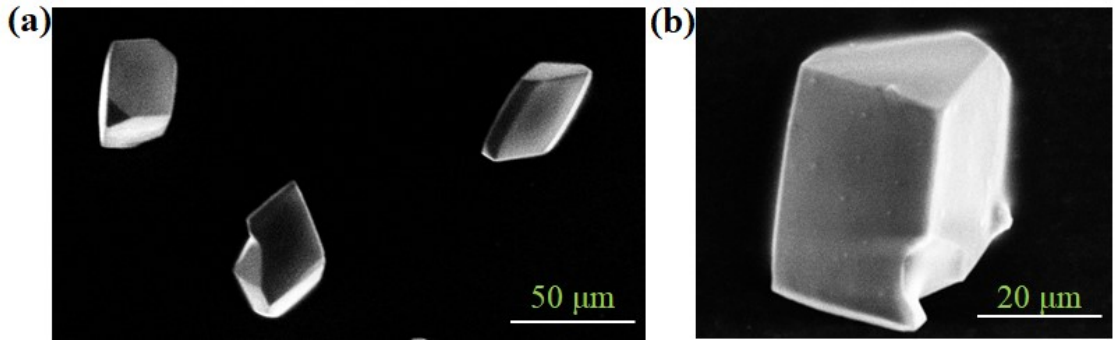

Figure S1 SEM images of **1**.

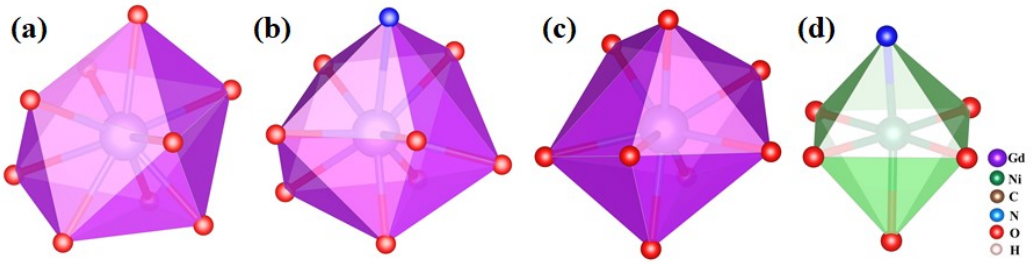

Figure S2 The coordination mode of Gd^{3+} and Ni^{2+} in **1**. (a) [GdO_9] polyhedron; (b) [GdO_8N] polyhedron; (c) [GdO_8] polyhedron; (d) [NiO_5N] polyhedron.

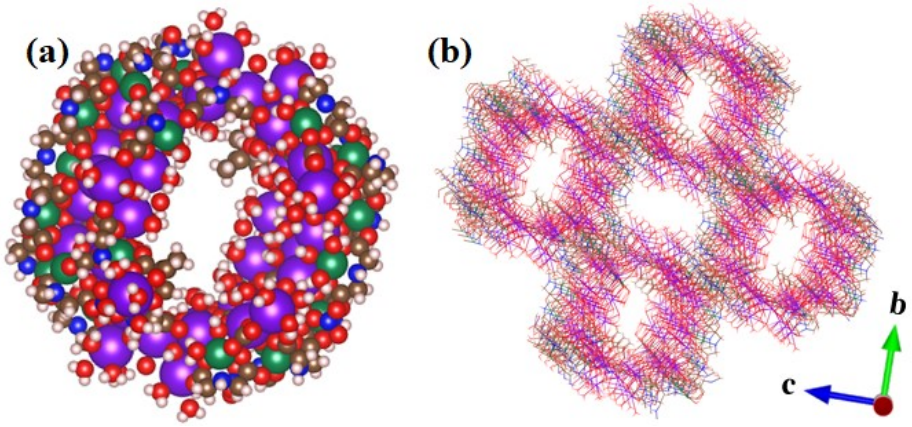

Figure S3 (a) The space-filling view of **1**; (b) Wireframe view of the packing mode of **1** aggregation.

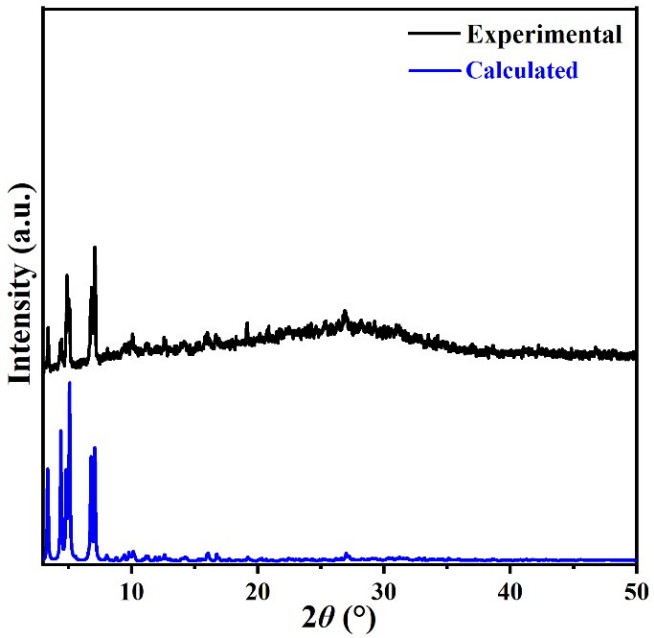

Figure S4 Calculated and experimental XRD patterns for **1**. The red curve is the calculated one obtained from single-crystal X-ray structure analysis.

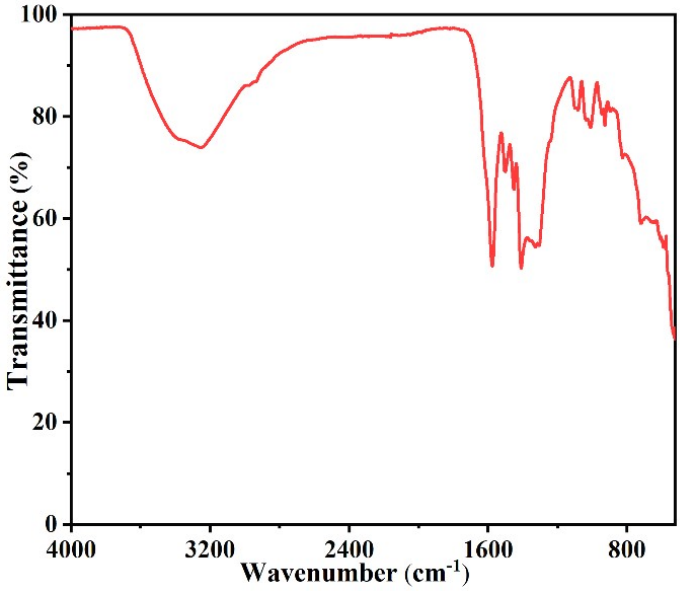

Figure S5 FTIR spectra of **1**.

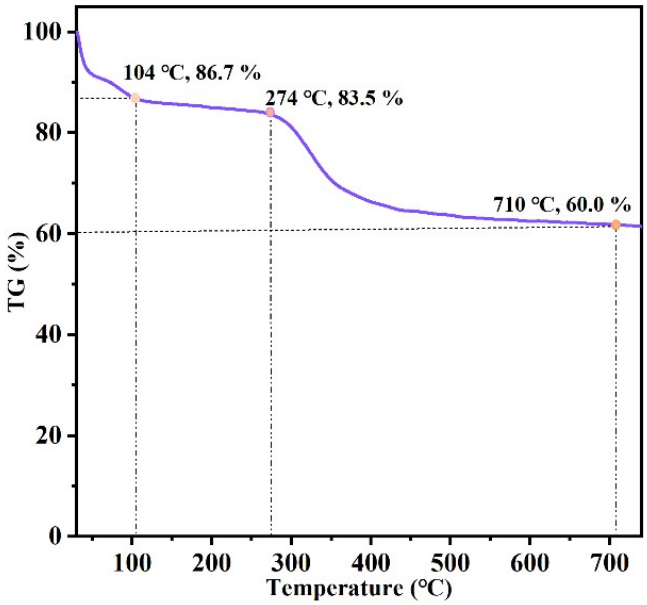

Figure S6 The thermogravimetric (TG) analysis of **1**.

Note: The TGA curve of **1** was investigated under N_2 atmosphere. The weight loss from room temperature to 104 ℃ should be attributed to the departure of guest molecules, and the calculated loss is 12.9 % while the observed loss is 13.3 %. With the temperature increasing, the coordinated water molecules, nitrate and acetate ligands are gradually lost and the cluster starts to decompose.The residue with the weight of 60.0 % at 710 ℃ is considered as metallic oxide (Gd_2O_3, NiO).

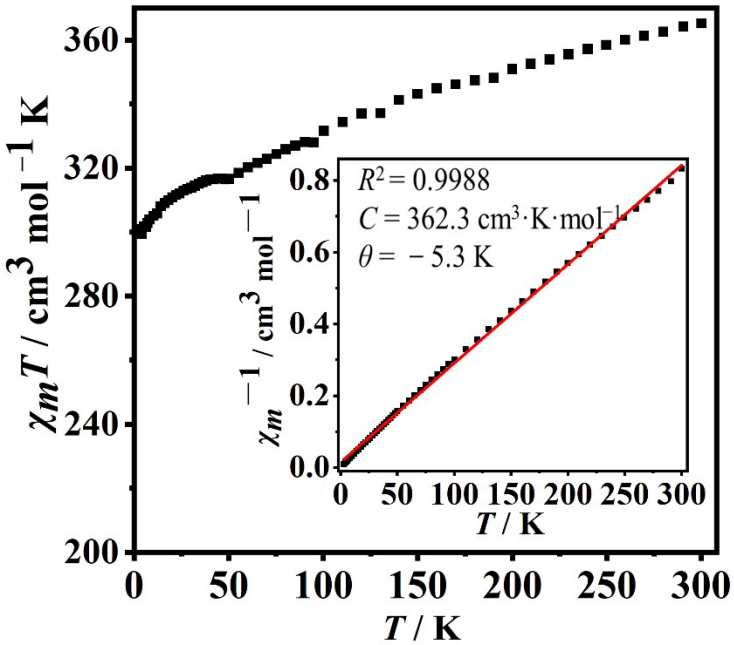

Figure S7. Plots of temperature dependence of $\chi_m T$ vs T and χ_M^{-1} vs T (inset) of wheel-like $\{Gd_{44}Ni_{22}\}$ cluster.

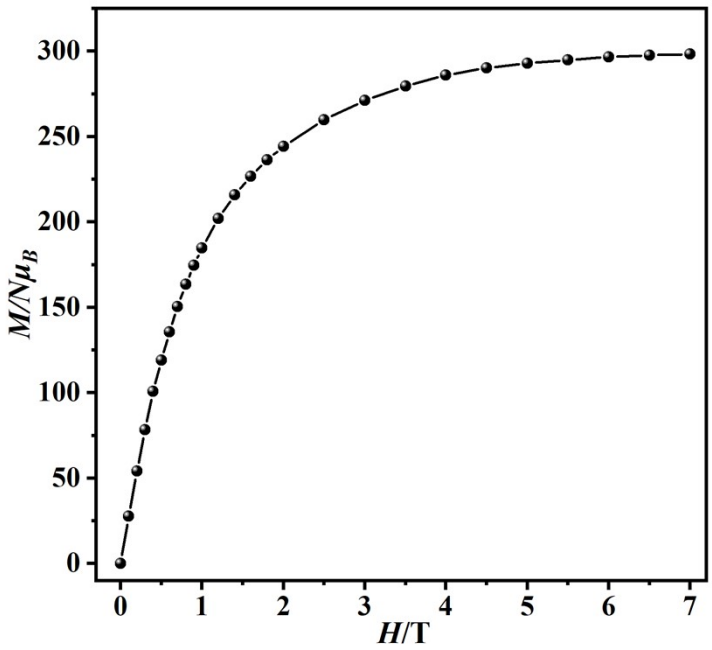

Figure S8 Experimental magnetization curve of **1** at 2 K.

References

1 G.Sheldrick, Acta. *Crystlogr. A. Found. Crystlogr.*, 2008, **64**, 112–122

2 O. Dolomanov, A. Blake, N. Champness and M. Schroder, Champness and M. Schroder, OLEX: new software for visualization and analysis of extended crystal structures, *J. Appl. Crystallogr.*, 2003, **36**, 1283–1284.

3 A. L. Spek, Single-crystal structure validation with the program PLATON, *J. Appl. Cryst.*, 2003, **36**, 7–11.

4 A. L. Spek, Structure validation in chemical crystallography, *Acta Cryst.*, 2009, **D65**, 148–155.

5 A. L. Spek, What makes a crystal structure report valid? *Inorg. Chim. Acta*, 2018, **470**, 232–237.

6 A. L. Spek, checkCIF validation ALERTS: what they mean and how to respond, *Acta Cryst.*, 2020, **E76**, 1–11.

7 X. M. Luo, Z. B. Hu, Q. F. Lin, W. W. Cheng, J. P. Cao, C. H. Cui, H. Mei, Y. Song and Y. Xu, Exploring the performance improvement of magnetocaloric effect based Gd-exclusive cluster Gd_{60}, *J. Am. Chem. Soc.*, 2018, **140**, 11219−11222.

8 J. B. Peng, X. J. Kong, Q. C. Zhang, M. Orendac, J. Prokleska, Y. P. Ren, L. S. Long, Z. Zheng and L. S. Zheng, Beauty, symmetry, and magnetocaloric effect four-shell keplerates with 104 lanthanide atoms, *J. Am. Chem. Soc.*, 2014, **136**, 17938−17941.

9 L. X. Chang, G. Xing, L. Wang, P. Cheng and B. Zhao, A 24-Gd nanocapsule with a large magnetocaloric effect, *Chem. Commun.*, 2013, **49**, 1055−1057.

10 F. S. Guo, Y. C. Chen, L. L. Mao, W. Q. Lin, J. D. Leng, R. Tarasenko, M. Orendá č , J. Prokleš ka, V. Sechovsky and M. L. Tong, Anion-templated assembly and magnetocaloric properties of a nanoscale $\{Gd_{38}\}$ cage versus a $\{Gd_{48}\}$ barrel, *Chem. Eur. J.*, 2013, **19**,

14876−14885.

11 X. Y. Zheng, J. B. Peng, X. J. Kong, L. S. Long and L. S. Zheng, Mixed-anion templated cage-like lanthanide clusters: Gd_{27} and Dy_{27}, *Inorg. Chem. Front.*, 2016, **3**, 320−325.

12 M. Y. Wu, F. L. Jiang, X. J. Kong, D. Q. Yuan, L. S. Long, S. A. AlThabaiti and M. C. Hong, Two polymeric 36-metal pure lanthanide nanosize clusters, *Chem. Sci.*, 2013, **4**, 3104−3109.

13 Y. Zhou, X.Y. Zheng, J. Cai, Z. F. Hong, Z. H. Yan, X. J. Kong, Y. P. Ren, L. S. Long and L. S. Zheng, Three giant lanthanide clusters Ln_{37} (Ln = Gd, Tb, and Eu) featuring a double-cage structure, *Inorg. Chem.*, 2017, **56**, 2037−2041.

14 X. Y. Zheng, Y. H. Jiang, G. L. Zhuang, D. P. Liu, H. G. Liao, X. J. Kong, L. S. Long and L. S. Zheng, A gigantic molecular wheel of $\{Gd_{140}\}$: a new member of the molecular wheel family, *J. Am. Chem. Soc.*, 2017, **139**, 18178−18181.

15 F. S. Guo, Y. C. Chen, L. L. Mao, W. Q. Lin, J. D. Leng, R.Tarasenko, M. Orendáč, J. Prokleš ka, V. Sechovsky and M. L. Tong, Anion-templated assembly and magnetocaloric properties of a nanoscale $\{Gd_{38}\}$ cage versus a $\{Gd_{48}\}$ barrel, *Chem. Eur. J.*, 2013, **19**, 14876−14885.

16 N. F. Li, X. M. Min, J. Wang, J. L. Wang, Y. Song, H. Mei and Y. Xu, Largest 3*d*-4*f* 196-nuclear $Gd_{158}Co_{38}$ clusters with excellent magnetic cooling, *Sci China Chem*, 2022, **65**, 1577–1583.

17 H. J. Lun, L. Xu, X. J. Kong, L. S. Long and L. S. Zheng, A high-symmetry double-shell $Gd_{30}Co_{12}$ cluster exhibiting a large magnetocaloric effect, *Inorg. Chem.*, 2021, **60**, 10079–10083.

18 W. P. Chen, P. Q. Liao, Y. Yu, Z. Zheng, X. M. Chen and Y. Z. Zheng, A mixed-ligand approach for a gigantic and hollow heterometallic cage $\{Ni_{64}RE_{96}\}$ for gas separation and magnetic cooling applications, *Angew. Chem., Int. Ed.*, 2016, **55**, 9375−9379.

19 W. P. Chen, P. Q. Liao, P. B. Jin, L. Zhang, B. K. Ling, S. C. Wang, Y. T. Chan, X. M. Chen and Y. Z. Zheng, The gigantic $\{Ni_{36}Gd_{102}\}$ hexagon: a sulfate-templated "star-of-david" for photocatalytic CO_2 reduction and magnetic cooling, *J. Am. Chem. Soc.*, 2020, **142**, 4663−4670.

20 J. B. Peng, Q. C. Zhang, X. J. Kong, Y. Z. Zheng, Y. P. Ren, L. S. Long, R. B. Huang, L. S. Zheng and Z. P. Zheng, High-nuclearity 3*d*–4*f* clusters as enhanced magnetic coolers and molecular magnets, *J. Am. Chem. Soc.*, 2012, **134**, 3314−3317.

21 Q. F. Lin, J. Li, X. M. Luo, C. H. Cui, Y. Song and Y. Xu, Incorporation of silicon–oxygen tetrahedron into novel high-nuclearity nanosized 3*d*–4*f* heterometallic clusters, *Inorg.Chem.*, 2018, **57**, 4799−4802.

22 D. P. Liu, X. P. Lin, H. Zhang, X. Y. Zheng, G. L. Zhuang, X. J. Kong, L. S. Long and L. S. Zheng, Magnetic properties of a single-molecule lanthanide–transition-metal compound containing 52 gadolinium and 56 nickel atoms, *Angew. Chem. Int. Ed.*, 2016, **55**, 4532−4536.

23 S. Fan, S. H. Xu, X. Y. Zheng, Z. H. Yan, X. J. Kong, L. S. Long and L. S. Long, Four 3d–4f heterometallic $Ln_{45}M_7$ clusters protected by mixed ligands, *CrystEngComm*, 2018, **20**, 2120−2125.

24 Z. M. Zhang, L. Y. Pan, W. Q. Lin, J. D. Leng, F. S. Guo, Y. C. Chen, J. L. Liu and M. L. Tong, Wheel-shaped nanoscale 3*d*–4*f* $\{Co^{II}_{16}Ln^{III}_{24}\}$ clusters (Ln= Dy and Gd), *Chem. Commun.*, 2013, **49**, 8081-8083.

25 J. D. Leng, J. L. Liu and M. L. Tong, Unique nanoscale $\{Cu^{II}_{36}Ln^{III}_{24}\}$(Ln= Dy and Gd)

metallo-rings, *Chem.Commun.*, 2012, **48**, 5286–5288.